BUCKLING AND GEOMETRIC NONLINEAR ANALYSIS OF A TIE ROD IN MSC/NASTRAN VERSION 68

by

George Campbell, Wen Ting
Light Truck Division, Ford Motor Company

Peyman Aghssa, Claus C. Hoff
The MacNeal-Schwendler Corporartion

ABSTRACT

The improved geometric nonlinear capability in MSC/NASTRAN Version 68 is tested on a large scale finite element model of a tie rod. The static buckling load of a tie rod is analyzed. The results of the finite element model are compared with experimental results. The analysis is performed in three steps. First, linear buckling is analyzed with SOL 105. Second, a nonlinear static analysis with arc-length method is performed in SOL 106 to determine the instability behavior of the structure. In the last step, a nonlinear buckling analysis is done with restart into SOL 106 to determine the nonlinear buckling load. The tie rod has a strongly nonlinear behavior which is due to material yield and geometric nonlinear effects. It is shown that MSC/NASTRAN's computed buckling load agrees well with the experimental buckling load.

Introduction

Linear buckling analysis and geometric nonlinear analysis with shell elements had problems in MSC/NASTRAN prior to Version 68. Users have observed higher order spurious modes in linear buckling analysis of thin shells using versions prior to Version 68. Furthermore, unsatisfactory convergence behavior of shell elements in geometric nonlinear analysis has been experienced in versions prior to Version 68.

Linear buckling and geometric nonlinear analysis with QUAD4 and TRIA3 shell elements have been improved in Version 68. The underlying theory of the improvements is discussed in references [1] to [5]. Some small test examples in [1] and [6] demonstrate that Version 68 is much more capable in buckling and geometric nonlinear analysis than the foregoing versions. In Version 68, the eigenvalue spectrum in linear buckling is free of spurious modes. Linear buckling is more reliable and easier to use in Version 68. The convergence behavior in geometric nonlinear analysis has been improved significantly in Version 68 compared to earlier versions. The CPU time in Version 68 is reduced up to one third of the CPU time of V67.5. Furthermore, problems converge which could not be solved before.

Until now, the improvements in Version 68 had not been applied to large scale models. This paper presents one of the first real life applications of the improved capabilities in Version 68. The ultimate load of a tie rod is calculated using buckling and geometric nonlinear capability of Version 68. The tie rod is modeled with mostly solid elements for the full cross sections and shell elements for the ring cross sections.

First, a brief summary of the theory is given. The emphasis of this paper is on the nonlinear analysis of a tie rod. The tie rod is analyzed in three steps. A linear buckling analysis is performed first. Then, a nonlinear static analysis with arc-length method is run to explore the stability behavior of the structure. The last step is a nonlinear buckling analysis. The numerical results are compared to experimental results.

Geometric Nonlinearity in MSC/NASTRAN

All nonlinear elements except the hyperelastic elements in MSC/NASTRAN use the so called corotational formulation in geometric nonlinear analysis. The average rigid body motion of a finite element is condensed out of the total deformations and only the remaining net deformations (distortions) are considered to calculate strains in the element. If we assume that the element net distortions remain small, a linear strain measure in the element is sufficient even for large overall deformations. The main task in the corotational formulation is the correct linearization of the virtual work of the internal forces in closed

form. The virtual work of the internal forces is

$$\delta W_{INT} = \delta \mathbf{d}_{(b)}^T \, \mathbf{f}_{(b)} \tag{1}$$

where $\delta \mathbf{d}_{(b)}$ are the virtual deformations (displacements and rotations) and $\mathbf{f}_{(b)}$ are the internal forces (normal forces and moments). The subscript (b) indicates components in basic. In the corotational formulation, internal element forces $\bar{\mathbf{f}}$ are evaluated from element net deformations $\bar{\mathbf{d}}$. The net deformations are the total deformations minus the element rigid body motion. The virtual work in terms of the internal element forces $\bar{\mathbf{f}}$ is

$$\delta W_{INT} = \delta \mathbf{d}_{(b)}^T \, \mathbf{T}_{bd} \, \mathbf{P}_{(d)}^T \, \bar{\mathbf{f}}_{(d)} \tag{2}$$

with

$$\mathbf{P}_{(d)} = \frac{\partial \bar{\mathbf{d}}_{(d)}}{\partial \mathbf{d}_{(d)}} \tag{3}$$

where $\mathbf{T}_{bd}$ is the transformation from basic to deformed element system, and the subscript (d) indicates components in the deformed element system. The partial derivatives in the correction matrix $\mathbf{P}_{(d)}$ are derived in [2] and [4].

The tangent stiffness is defined to be the derivative of the internal forces with respect to the deformations

$$\mathbf{K}_{(b)} := \frac{\partial \mathbf{f}_{(b)}}{\partial \mathbf{d}_{(b)}} \tag{4}$$

The tangent stiffness matrix is derived from the second variation of the virtual work (2). In MSC/NASTRAN, the tangent stiffness is calculated by adding the linear or nonlinear material stiffness $\overline{\mathbf{K}}$ to the differential stiffness $\mathbf{K}_D$,

$$\mathbf{K}_{(b)} = \mathbf{T}_{bd} \left(\mathbf{P}_{(d)}^T \overline{\mathbf{K}}_{(d)} \, \mathbf{P}_{(d)} + \mathbf{K}_{(d)}^D \right) \mathbf{T}_{bd}^T \tag{5}$$

with

$$\overline{\mathbf{K}}_{(d)} = \frac{\partial \bar{\mathbf{f}}_{(d)}}{\partial \bar{\mathbf{d}}_{(d)}} \tag{6}$$

The linear or nonlinear material stiffness contains the terms due to the variation of the stresses. The differential stiffness contains the terms due to the variation of the strains, it is often called the geometric stiffness. For geometric linear problems, the correction matrix $\mathbf{P}_{(d)}$ becomes the identity matrix.

Buckling Analysis of a Tie Rod

Description of the Problem

The buckling load of a tie rod has to be determined. The geometry of the tie rod is shown in Figure 1. The material is steel. The steel has elasto-plastic behavior with hardening. Due to material cold work, the yield stress varies over the length of the tie rod, see Figure 2.

For the computational model, we assume von-Mises elasto-plastic material law with isotropic hardening, see Figure 2. The tie rod is modeled with HEXA8 and PENTA6 solid elements in areas with full cross sections. QUAD4 and TRIA3 shell elements are used to model the ring cross sections. The tie rod is simply supported at the two ends. The finite element model is shown in Figure 3.

Buckling Test

The tie rod is axially loaded, see Figure 4. Five samples have been tested, the measured buckling loads are listed in Table 1. The average buckling load of the 5 tests is 21.04 kN with a variance of 0.66 kN. In Figure 5, tie rod sample 2 is shown before and after the buckling test. The tie rod deformed mainly in the bend area. The results of the buckling tests are a courtesy of TRW Canada Limited.

Computational Analysis

We perform the analysis in three steps.

- Linear buckling analysis is made to check the model and to examine the type of buckling mode.
- Nonlinear static analysis with arc-length method is done to examine the buckling and post-buckling path of the load deflection curve.
- A restart is made into the nonlinear static solution to perform a nonlinear buckling analysis.

Linear Buckling Analysis

SOL 105 is used to determine the first linear buckling load and mode shape. The analysis is restricted to linear elastic material and infinitesimal deformations. The static axial load is applied in the first subcase. The following eigenvalue problem is solved in the second subcase,

$$\left(\mathbf{K} - \lambda_i \mathbf{K}^D\right) \mathbf{x}_i = \mathbf{0} \tag{7}$$

where $\mathbf{K}$ is the linear stiffness, $\mathbf{K}^D$ is the differential or geometric stiffness which is a function of stresses due to the static load $\mathbf{P}$ from the first subcase. The problem (7) is solved for the eigenvalues λ_i and eigenvectors $\mathbf{x}_i$. The critical buckling loads are

$$\mathbf{P}^i_{crit} = \lambda_i \mathbf{P} \tag{8}$$

The first buckling mode is shown in Figure 6. The first critical buckling load from linear buckling in Version 68 is

$$\mathbf{P}_{crit} = 72.1 \text{ [kN]} \qquad \text{SOL 105 Buckling Load} \tag{9}$$

Note that the linear buckling analysis with the Pre-Version 68 method gives negative eigenvalues because spurious modes in thin shell elements spoil the eigenspectrum (see explanations above).

First, we compare the result of the computation with the Euler buckling load of a simply supported straight beam

$$\mathbf{P}_{crit} = \frac{\pi^2}{l^2} EI \tag{10}$$

where l is the length of the beam, E is the Young's modulus and I is the area moment of inertia

$$I = \frac{1}{64}\pi D^4 \tag{11}$$

where D is the diameter of the circular cross section. With $D \approx 20mm$, $l \approx 420mm$ and $E \approx 207,000N/mm^2$, the critical Euler buckling load is

$$\mathbf{P}_{crit} = 91.0 \text{ [kN]} \qquad \text{Euler Buckling Load} \tag{12}$$

Compared to the Euler buckling load, the linear buckling load of SOL 105 appears to be a realistic value. Note that the Euler buckling load is a rough estimate which does not account for the curved shape and the change in the cross section over the length.

Compared to the test, the linear buckling load is about 3.6 times higher than the experimental buckling load. The first buckling mode from linear analysis does not agree with the buckling shape of the experiment, see Figure 5 and 6. The results indicate that a linear analysis is not realistic to simulate the failure of the tie rod. Nonlinear effects have to be taken into account to match the experimental buckling load with the buckling load of the finite element model.

Nonlinear Static Analysis

Potential nonlinear effects are the yielding of the material and the geometric softening effect due to the curved shape of the tie rod. Therefore, we run nonlinear static analysis with material and geometric nonlinearities turned on.

In the first SOL 106 run, we want to simulate the load deflection path up to the buckling load and beyond. In the first subcase, we load the structure up to 18.0 kN using the modified Newton method. In the second subcase, we switch from load control to arc-length method to follow the load deflection curve in the vicinity of the buckling load. Modified Riks with combined load and displacement control is chosen. The maximum in the load deflection curve is reached at a load of

$$\mathbf{P}_{max} = 23.034 \text{ [kN]} \tag{13}$$

At this point, a negative factor diagonal in the stiffness matrix is encountered for the first time in the load history. Thereafter, the structure continues to deform in the post-buckling branch, the arc-length method reduces the load with increasing displacements, see the load-deflection curve in Figure 7. The deformation of the tie rod at the maximum load is shown in Figure 8. The maximum in the load deflection curve and the negative factor diagonal of the stiffness indicate that a buckling point is reached. The deformed shape from nonlinear analysis is in good agreement with the deformed shape of the test samples, see Figure 5 and 8.

Nonlinear Buckling Analysis

A restart into SOL 106 is made to perform a nonlinear buckling analysis. The nonlinear buckling analysis will provide a more accurate buckling load and furthermore we get the buckling shape and higher order buckling loads and shapes. In nonlinear buckling, the following eigenvalue problem is solved

$$(\mathbf{K}_n + \lambda_i \Delta\mathbf{K})\mathbf{x}_i = \mathbf{0} \tag{14}$$

with

$$\Delta\mathbf{K} = \mathbf{K}_n - \mathbf{K}_{n-1} \tag{15}$$

where $\mathbf{K}_n$, $\mathbf{K}_{n-1}$ are tangent stiffness matrices at load step n and n-1, respectively. The critical buckling load is

$$\mathbf{P}_{crit} = \mathbf{P}_n + \alpha\Delta\mathbf{P} \tag{16}$$

with

$$\Delta\mathbf{P} = \mathbf{P}_n - \mathbf{P}_{n-1} \tag{17}$$

The factor α is calculated from

$$\alpha = \frac{\lambda_i \Delta \mathbf{u}^T (\mathbf{K}_n + \frac{1}{2}\lambda_i \Delta \mathbf{K})\, \Delta \mathbf{u}}{\Delta \mathbf{u}^T \Delta \mathbf{P}} \tag{18}$$

with

$$\Delta \mathbf{u} = \mathbf{u}_n - \mathbf{u}_{n-1} \tag{19}$$

We restart from a load of $22.900\,kN$ and increase the load in two steps to $23.000\,kN$. With $\Delta P = 0.050\,kN$, the eigenvalue analaysis gives a critical load factor of $\alpha = 0.05$. The critical nonlinear buckling load is

$$\mathbf{P}_{crit} = 23.003\ [\mathrm{kN}] \tag{20}$$

Summary of the Analysis

It has been shown that we can not match the critical buckling load with linear buckling analysis. The critical load from linear buckling analysis is much higher than the experimental buckling load. The tie rod behaves strongly nonlinear. Both nonlinear static and nonlinear buckling analysis give a buckling load which is close to the experimental buckling load. The finite element model overestimates the buckling load by about 9%.

Concluding Remarks

The procedure which we have used in this paper may serve as a general guideline for nonlinear buckling analysis. However, we have to make two additional remarks with regard to general applications.

- We used some a priori knowledge in the first nonlinear static run. Knowing the experimental buckling load, we load the structure up to about 80% of the observed buckling load and use arc-length method thereafter. The purpose is to make the analysis more efficient by avoiding small load steps for load levels lower than the buckling load. If there is no experimental data available, we recommend to run the nonlinear static analysis up to 80% of the linear buckling load and watch for the first occurence of a negative factor diagonal in the stiffness.
- We have to mention here that the initial shape of the tie rod has significant components of the first buckling mode. Therefore, the nonlinear static analysis deforms

automatically in the first buckling mode. We do not have to deal with bifurcation and branch switching problems in this example. Additional measures must be taken for structures which start with a shape which has no component of the first buckling mode. An initial perturbation in the direction of the first buckling mode has to be introduced to force the structure into the load deflection path which corresponds to the first buckling load.

The paper shows that nonlinear analysis with MSC/NASTRAN Version 68 is capable enough to solve complex nonlinear problems with large scale models.

References

1. Hoff, C.C.," Improvements in Linear Buckling and Geometric Nonlinear Analysis of MSC/NASTRAN's Lower Order Shell Elements ", MSC 1993 World Users' Conference, Arlington, Virginia, May 1993.

2. Hoff,C.C.," Software Requirement Specification for the QUAD4 Differential Stiffness ", MSC/NASTRAN Memo CCH-8, The MacNeal-Schwendler Corporation, Los Angeles, CA, January 1993.

3. MacNeal,R.H.," Critique of MSC/NASTRAN Large Displacement Capability ", MSC/NASTRAN Memo RHM-124B, The MacNeal-Schwendler Corporation, Los Angeles, CA, August 30, 1991.

4. Nour-Omid,B. and Rankin,C.C.," Finite Rotation Analysis and Consistent Linearization Using Projectors ", *Computer Methods in Applied Mechanics and Engineering* 93, 353-384, 1991.

5. Rankin,C.C. and Nour-Omid,B.," The Use of Projectors to Improve Finite Element Performance ", *Computers& Structures*, Vol.30, No.1/2, pp.257-267, 1988.

6. MSC/NASTRAN Version 68 Release Notes, The MacNeal-Schwendler Corporation, Los Angeles, CA, April 1994.

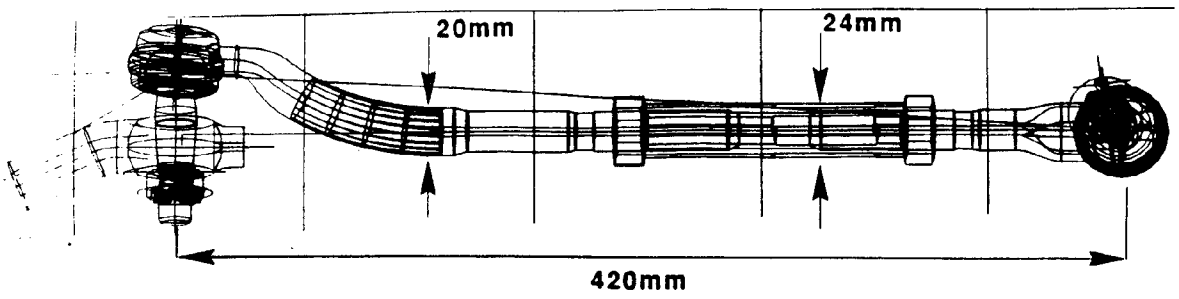

Figure 1. **Geometry of the tie rod.**

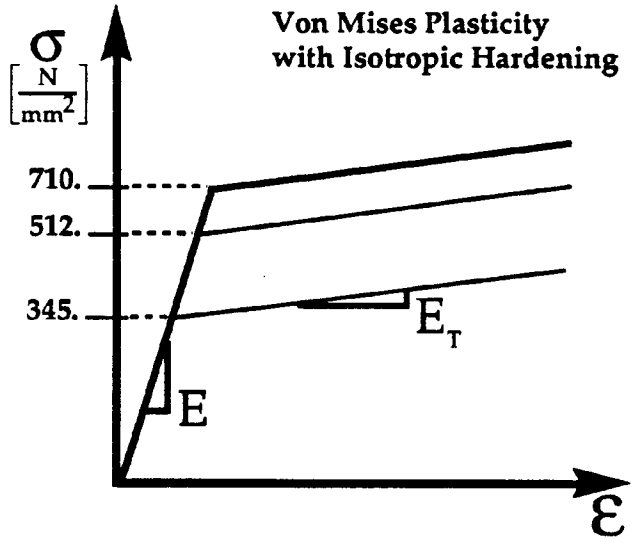

Youngs Modulus	$E = 2.07e5 \frac{N}{mm^2}$	
Hardening Slope	$E_T = 0.08 \bullet E$	
Yield Stress	$\sigma_y = 710 \frac{N}{mm^2}$	thread area
	$\sigma_y = 345 \frac{N}{mm^2}$	bend area
	$\sigma_y = 512 \frac{N}{mm^2}$	in between

Figure 2. **Material models of the tie rod.**

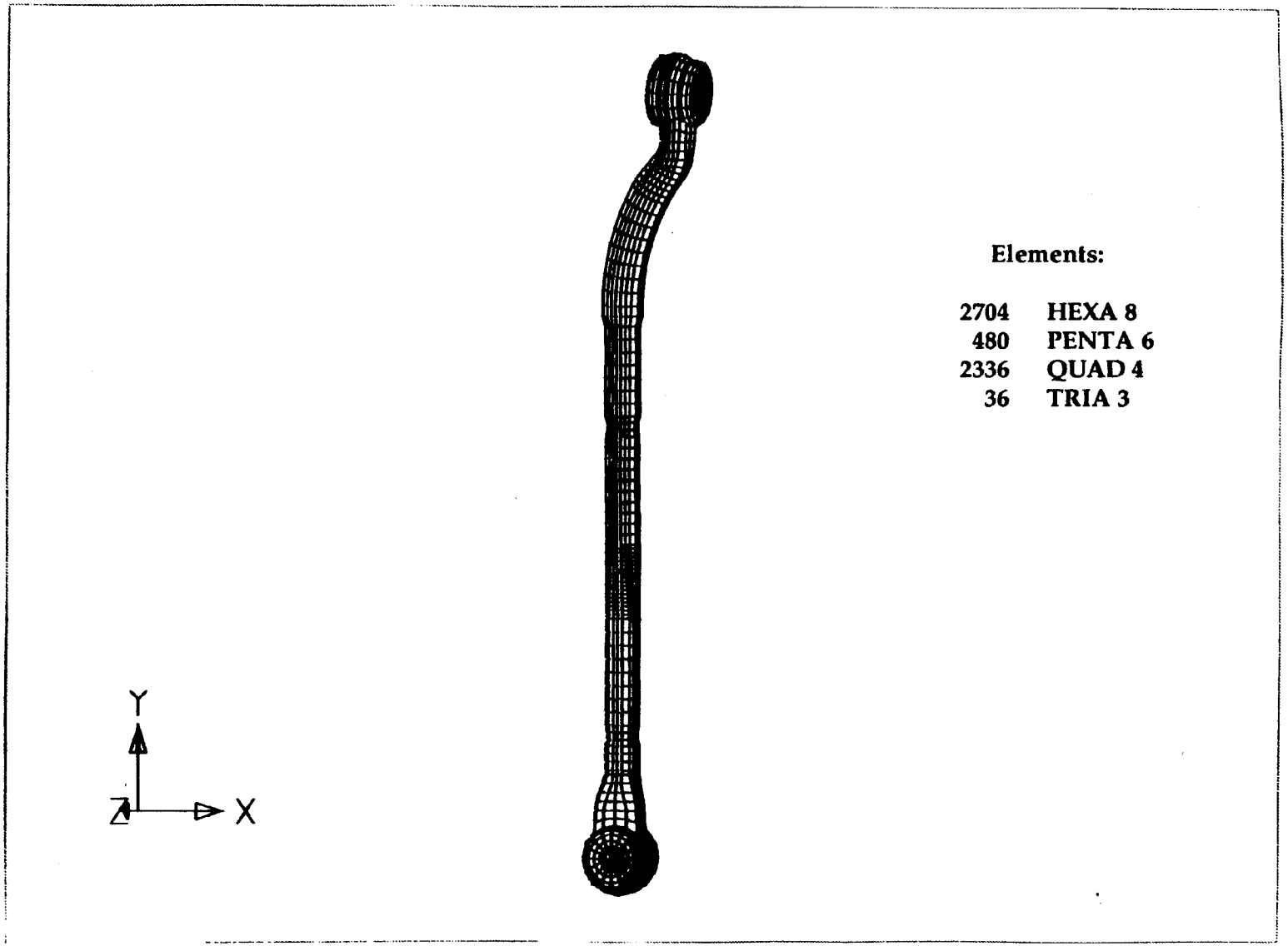

Figure 3. Finite element model of the tie rod

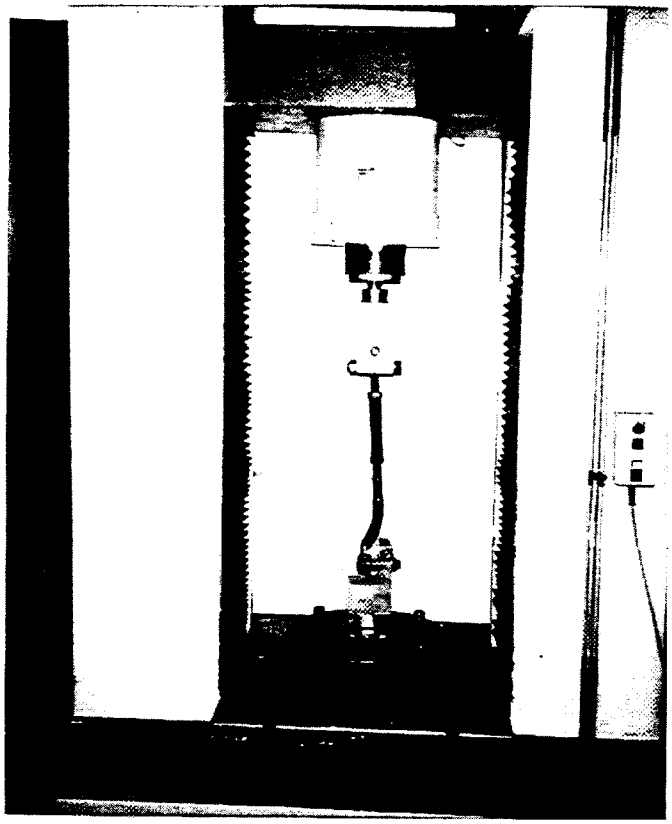

Figure 4. Buckling test for tie rod

Sample No	Load kN (Lbs)	Failure Mode
1295-01	21.7 (4878)	Bend
1295-02	21.7 (4878)	Bend
1295-03	20.9 (4698)	Bend
1295-04	19.9 (4474)	Bend
1295-05	21.0 (4721)	Bend

Table 1. Buckling test results

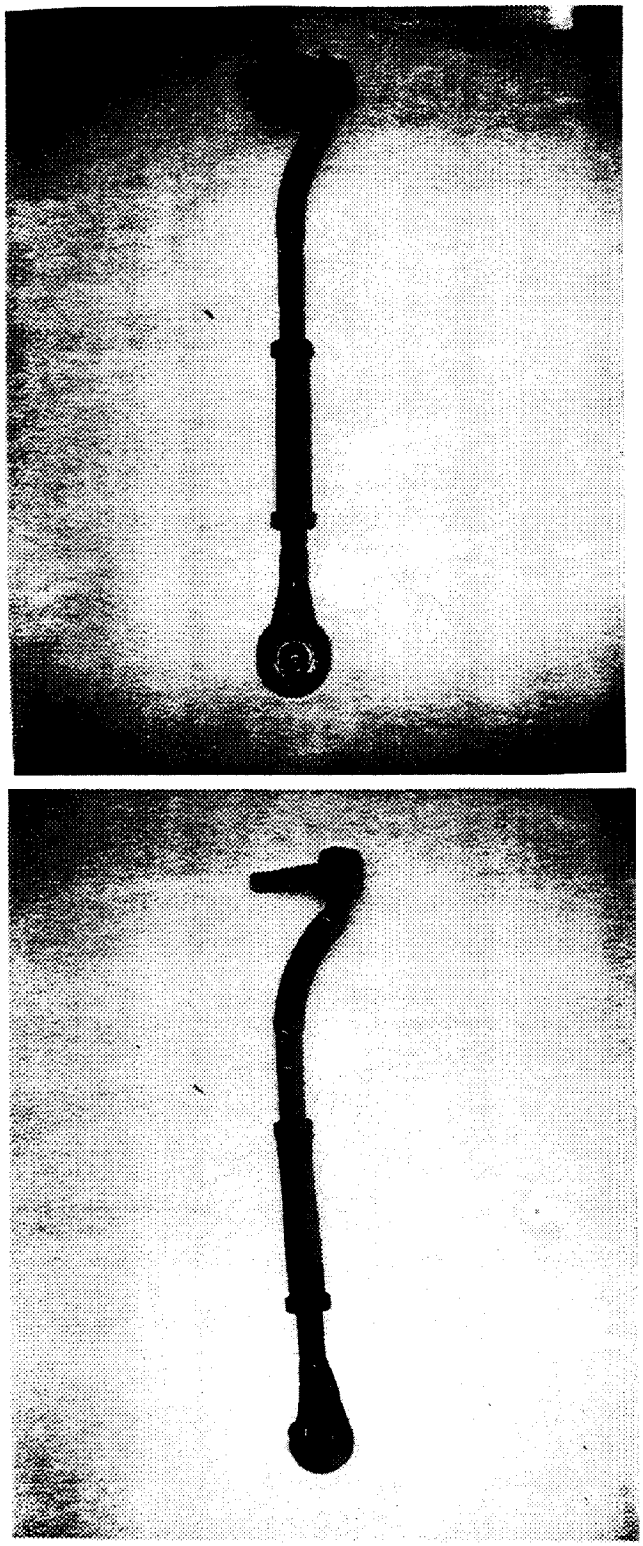

Undeformed

Deformed

Figure 5. Tie rod sample - Before and after the buckling test.

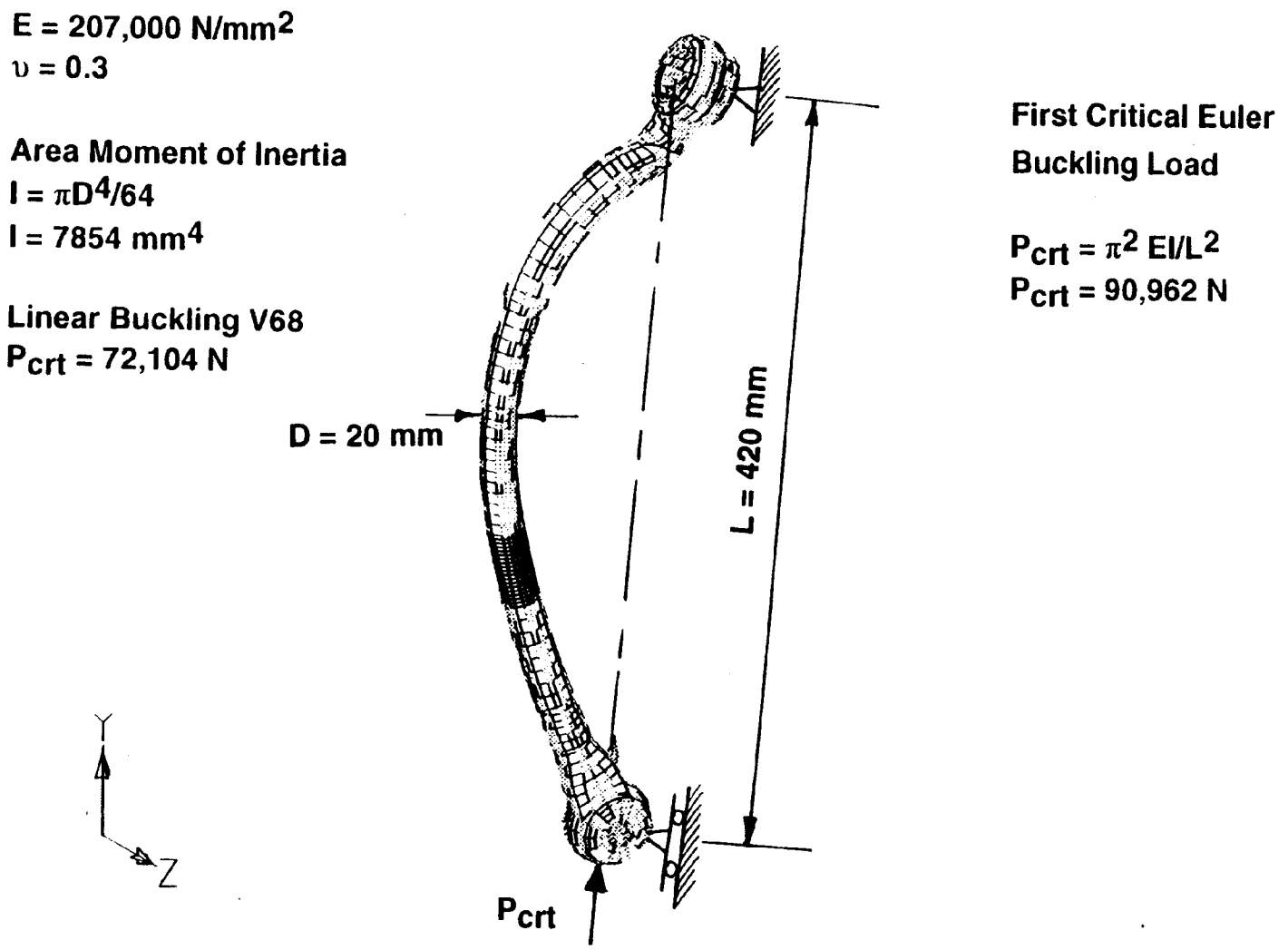

Figure 6. First buckling mode form linear buckling analysis

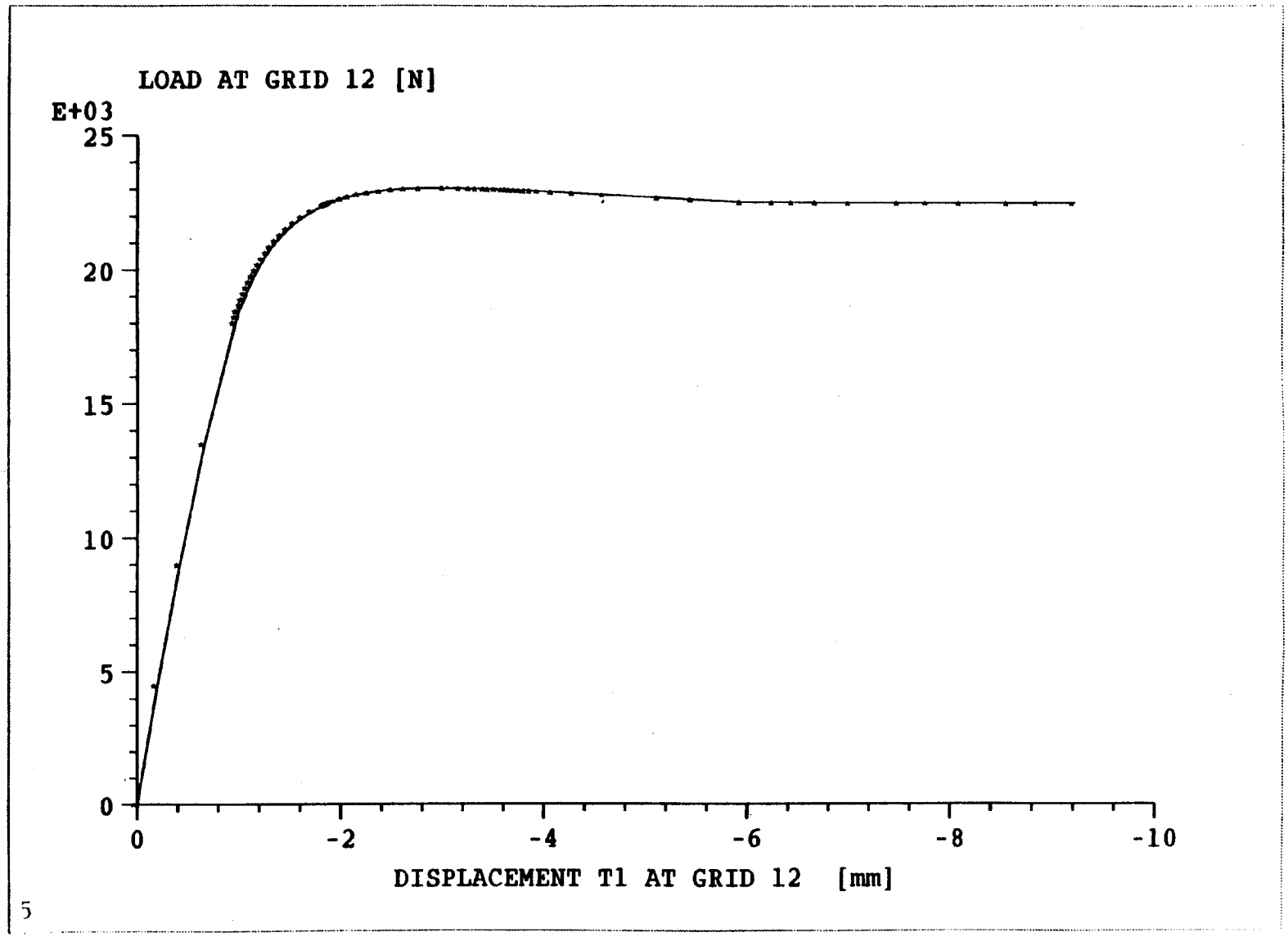

Figure 7. Computed load-deflection curve at grid point with applied concentrated force.

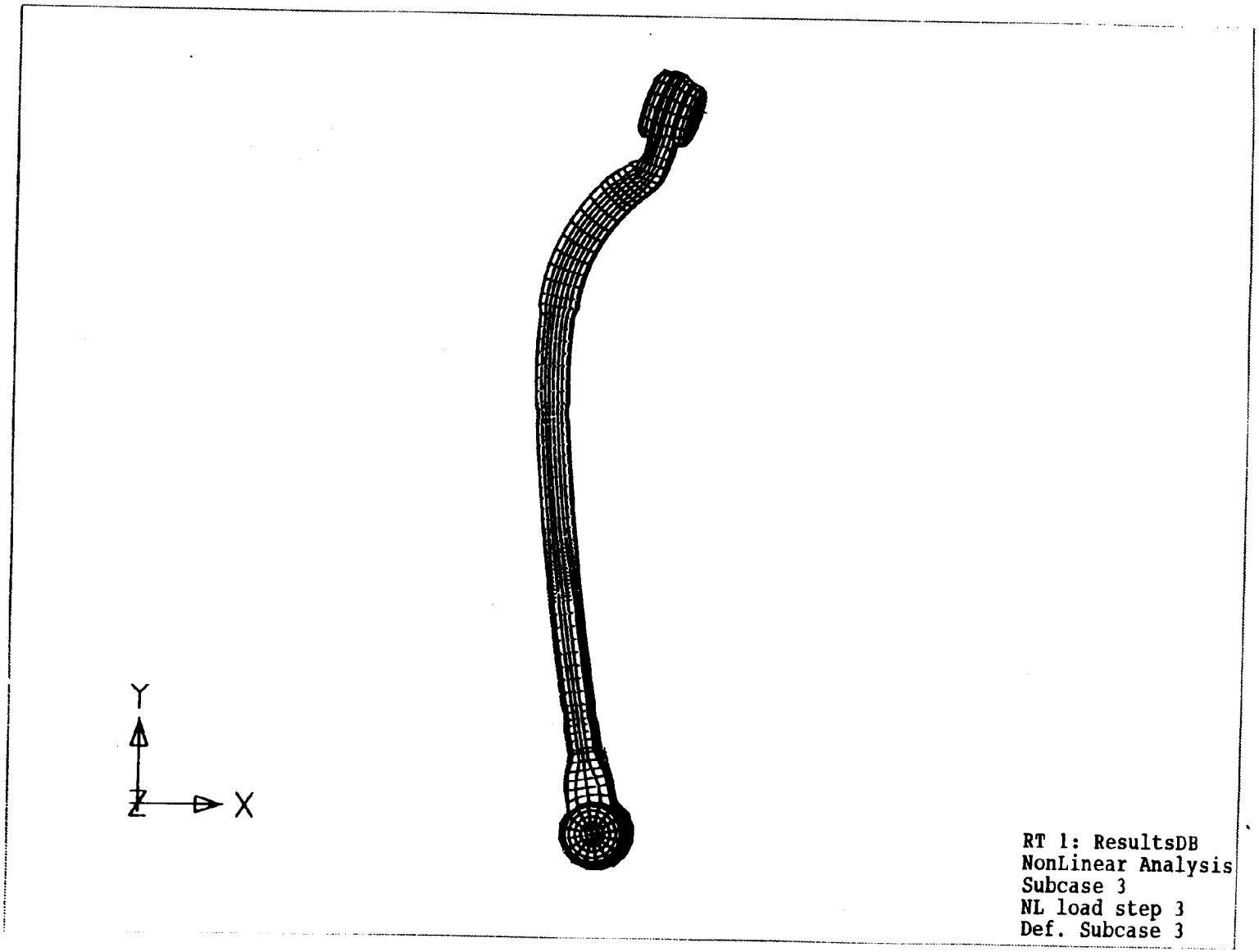

Figure 8. Computed deformation of the tie rod at the buckling load.